Adaptive Optics Testbed for the Visible High Resolution Imaging

Young Soo Choi*, Jae Eun Yoo, Seung Soo Kim
Agency for Defense Development, Yuseung P.O Box 35-3, Daejeon, 305-600, Republic of Korea

Won Tae Park, Jong Kyu Jung and Soo Man Lee
Electro Optics Center, R&D Division, Doosan DST, Republic of Korea

ABSTRACT

We have developed Adaptive Optics testbed to obtain the visible high resolution imaging. Here, the various experimental performances of the AO testbed in the laboratory have been reported. The closed-loop AO system with real-time operations that is 1000Hz sampling frequency, has been compensated for both tip/tilt and high order disturbances induced by the rotating phase plates as the atmospheric turbulence simulators. A 277-element Deformable mirror with continuous membrane magnetic voice coils is matched with a 20x20 Shack-Hartmann wavefront sensor. To evaluate the quality of the image, the average Strehl ratios have been measured as a function of object light levels and atmospheric seeing conditions.

1. INTRODUCTION

Until today, Adaptive Optics (AO) technologies have intensively developed to improve the correction of the optical distortion induced by the atmospheric turbulence in solar and astronomical observations, free space optical communications, imaging through the atmosphere and military defense [1-5]. Random optical distortions are produced by temporal and local variations in the refractive index or density of air that cause imaging blur in the light coming from space. In real-time wavefront compensation, AO technology corrects irregular atmospheric fluctuation or wavefront aberration that affected telescope image quality due to the atmospheric turbulence.
In general, AO system consists of a wavefront sensor (WFS), a wavefront corrector, and a control computer with high speed parallel signal processing modules. WFS senses the distorted wavefront by turbulence and measures the wavefront gradients. In the wavefront corrections, the disturbed wavefront is corrected by tip-tilt mirror (TTM) and deformable mirror (DM). The residual wavefront errors are measured by the WFS in the feedback AO closed-loop. To apply the control command signals to TTM and DM in the real-time, the control computer is operated with the reconstruction algorithm and the control algorithm. It is designed by FPGA (Field Programmable Gate Array) with high speed parallel computing capability. The drive voltage signals of TTM and DM are computed by the control computer for the wavefront compensation. Strehl ratio is measured to evaluate the quality of the image. According to the point spread function (PSF), it is defined by the ratio between the peak intensity of the Airy pattern of the closed-loop image and that of a perfect diffraction limit image for the same optical system [6].
In this study, the Strehl ratios after correction have been measured to evaluate the performances of AO testbed system in laboratory tests. We have analyzed them experimentally as a function of object light magnitudes and atmospheric seeing conditions such as Fried coherence length and wind speed in the rotating phase plates. Also, in field tests, we have carried out and tested the quality of the visible AO images in resolution by using USAF bar target at 1.15km.

2. SETUP OF ADAPTIVE OPTICS TESTBED

We have developed Adaptive Optics testbed system to obtain the visible image in high resolution with real-time operations. Fig 1 shows a photo and optical layout of the closed-loop AO testbed system with the atmospheric simulator, telescope simulator and light source simulator for the indoor laboratory experiments. The generating wavefront errors by a rotating phase plate are corrected by the AO testbed with 1000Hz sampling frequency. It is minimized in the feedback closed-loop compensations.
AO testbed system is consisted of the tilt compensation with tip-tilt mirror and tip-tilt sensor, the higher-order compensation with DM and Shack-Hartmann wavefront sensor (SH-WFS), the real-time control computer with high speed parallel computing capability and imaging camera. He-Ne laser (λ=633nm, HNL225R) is used as illuminating light source simulator. To produce random wavefront distortions, the atmospheric turbulence simulator is operated by the phase plate (Lexiteck Inc.) with rotating stage and stepper controller. It is placed in front of telescope

simulator. For various temporal Greenwood frequencies, the rotating speed of the phase plate is adjusted to simulate the different wind speeds. Telescope simulator is de-magnified by using the reflective lens of 20mm diameter for the 1.8m Bohyun astronomical telescope which is located at southeastern area of South Korea. It is scaled down on the primary mirror with a secondary mirror obscuration and spider supports.

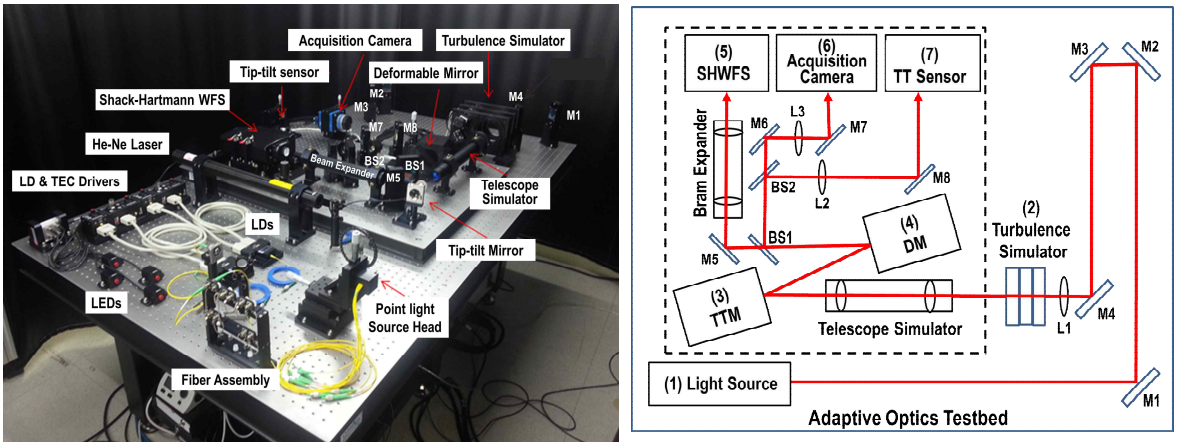

Fig 1. The setup view and optical layout of the closed-loop AO testbed system.

In AO testbed, the compensation of the wavefront error is performed separately by the tilt compensation with tip-tilt mirror and tip-tilt sensor and higher-order compensation with DM and SH-WFS. The tip-tilt mirror (S-330.2SL, Physik Instrumente) is 32 mm in diameter. The nominal 3dB banwidth of the TTM is measured at 180Hz. The mechanical dynamical range is ±1.5°. The tip-tilt sensor (TTS) is used CMOS camera (pco.edge4.2, PICO) which has more than 1000 frame rates in the image area of 150×150 pixels. It has 2048x2048 pixels at full resolution, and the pixel size of 6.5 ㎛. As the wavefront corrector for high-order compensation, DM (DM-277-15, Alpao) has with a voice coiled magnetic membrane as continuous facesheet mirror [7, 8]. It has the pupil diameter of 24.5mm with 277 actuators on a 1.5mm pitch. Also, it has the inter-actuator stroke of 5μm PV and 1200Hz bandwidth. It is matched with a Shack-Hartmann wavefront sensor (SH-WFS). SH-WFS consists of a 20x20 lenslet array and OCAM2 camera (Firstlight Imaging Inc.) with 1500 frame rate. Microlens array by fused silica is coated 400～1000nm range on the substrate. The pitch of the lenslet array is 288 ㎛ and the focal length is 22mm. The OCAM2 camera is used by the deep depletion EMCCD (Electron-multiplying charge-coupled Device) CCD220 detector [9-11]. The CCD220 detector (E2V) is a 24 ㎛ square 240x240 pixels split frame transfer back illuminated L3 Vision CCD. It is operated at –45℃, chilled by a liquid cooling circuit and a Peltier cooler. It is capable of 1500 fps with sub-electron readout noise. It is placed at the focal plane of the sub-apertures. DM is matched with effective 16x16 lenslet array of SH-WFS in use.

The control computer which includes high speed parallel signal processing (SPS) module is used to obtain the error vectors from the local wavefront slopes of SH-WFS, to run the wavefront reconstruction and to compute the control commands applied to the DM actuators in a feedback closed-loop. The reconstruction algorithm and the control algorithm are performed to calculate the drive voltages of DM and TTM. In the real-time control computer, the SPS module has five Field Programmable Gate Array (FPGA) boards (National Instrument) and a computer. It is done with NI's LabView environment for wavefront correction. One of the five FPGA's is assigned to measure TTS and calculate control signals for TTM, while the rest four are used to receive SHWFS signal, calculate slops for each subaperture and obtain the correction signal for DM. It has been operated more than 1 kHz wavefront correction speed in AO closed loop. The beamsplitter divides the SH-WFS path and the image camera path.

Imaging CCD camera (MR285MC-BH, XIMEA) has a resolution of 1320×1040 pixels and a pixel size of 6.45 ㎛. We have measured the Strehl ratio after corrections at various atmospheric turbulence conditions in the laboratory. Also, we have evaluated the quality of the image of USAF bar target after AO corrections in field test.

3. EXPERIMENTAL RESULTS

The experimental test results have been analyzed for the performance characteristics of AO testbed system. As atmospheric turbulence simulator, the phase plates have simulated various Fried coherence lengths and wind speeds. They have varied from under 8cm to more than 18cm at 633nm according to a Kolomogorov spatial frequency distribution. So, the effective turbulence parameter (D/r_o) ranges from 10 to 23. In the rotating phase plates, the wind speed has simulated up to 15m/sec. The Greenwood frequency as the characteristic turbulence rate ranges from 20 to 60Hz. The measured Strehl ratios have been recorded repeatedly by the average values of every successive 100 runs in the 1000Hz sampling during the AO operations. The wavefront measurement wavelength equals the observation wavelength.

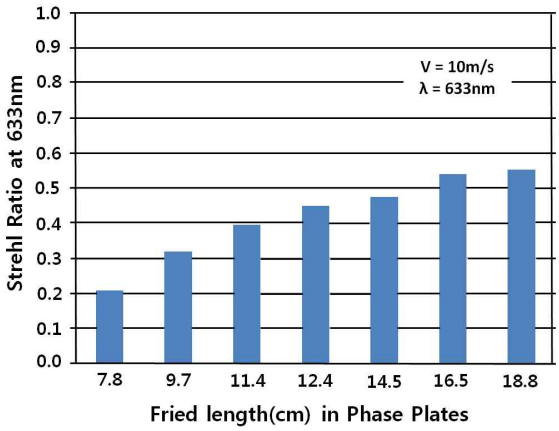

Fig 2. Strehl ratios vs. Fried coherence lengths of the phase plates.

After AO corrections, the average Strehl ratios at 633nm as a function of Fried coherence length of phase plates in the closed-loop AO testbed system is shown in Fig 2. At the various phase plates, the SR increases as Fried coherence length increases with constant wind speed of 10m/sec. The average SR was measured 0.21 and 0.47 for the Fried coherence length of 7.8 and 14.5cm at 633nm, respectively. As the turbulence increases, the Strehl ratio is decreased due to atmospheric fitting error and temporal Bandwidth error. Greenwood frequency is varied from 22.7 to 54.7Hz.

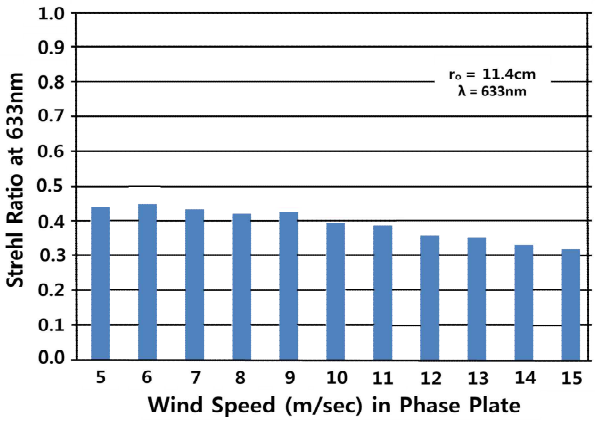

Fig. 3. Strehl ratios vs. wind speed of the phase plates

The average SR as a function of the wind speed of the rotating phase plate is shown in Fig 3 after correction in the closed-loop AO testbed system. As the wind speed increases in the rotating phase plate with constant Fried coherence length of 11.4cm, SR is decreased due to the temporal turbulence effects by high Greenwood frequency.

For a single turbulent layer moving at a speed v, Greenwood frequency f_G is written by $f_G = 0.427(v/r_{o)}$ as the characteristic turbulence rate. It ranges from 18.7Hz to 56.2Hz in these experiments. The residual wavefront variance of the characteristic change time of the turbulence, is expressed by $\sigma^2_{BW} = (f_G/f_{BW})^{5/3}$ where f_{BW} is the control bandwidth of AO system. It is increased as Greenwood frequency increases. So, SR decreases in high Greenwood frequency.

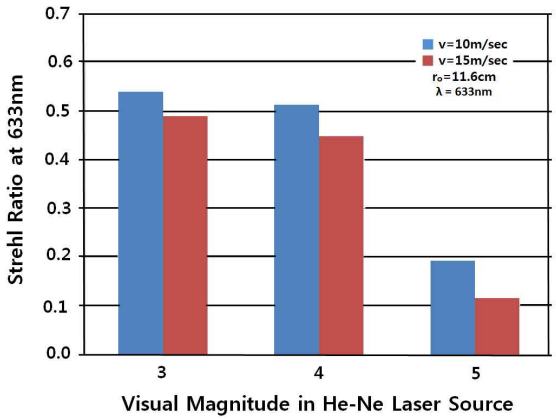

Fig 4. Strehl ratios vs. visual magnitude at 633nm

The average SR as a function of the visual magnitude at 633nm He-Ne laser in the closed-loop AO testbed system after correction is shown in Fig 4. In the phase plate with Fried coherence length of 11.4cm, SR has been operated 0.54 and 0.49 at 3rd magnitude for the wind speeds of 10m/s and 15m/sec, respectively. SR has been obtained 0.19 and 0.12 at 5th magnitude, respectively. As the visual magnitude increases, the Strehl ratio is decreased due to the wavefront sensor measurement error. In an enough bright source, the signal to noise ratio (SNR) of SHWFS is high. So, the measurement error of SH-WFS is inversely proportional to the SNR.

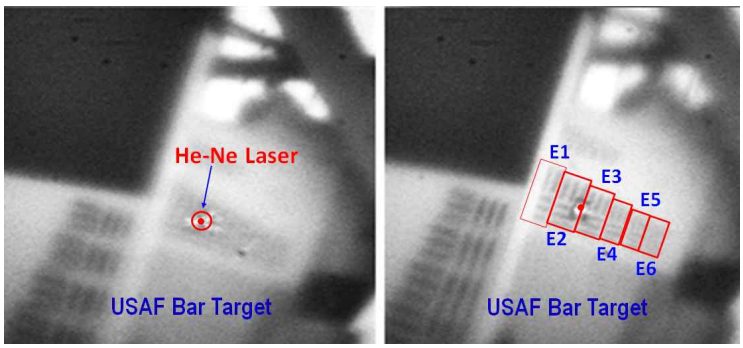

Fig 5. Image comparisons of USAF bar target before (a) and after AO correction (b) at 1.15km in the field

Image comparisons of USAF bar target before correction and after correction for AO correction is shown in Fig 5 in the field test. USAF bar target for resolution testing is located 1.15km away from the AO testbed in laboratory room with slant path. It is mounted on the middle of a tower of 10m height. To calculate the wavefront error, He-Ne laser has installed on back of USAF bar target with beam expander. It passes through the hole in the middle of USAF bar target. AO system was coupled of the 305mm telescope (LX200 ACE 12”). The reflected sun light of USAF target and He-Ne laser beam are collected by the telescope. The focal length of the telescope is 3048mm. The beam is collimated by articulated arm as a relay optics and is transferred to the AO testbed. The visible images of USAF bar target were obtained with black and white CCD imaging camera (XIMEA, MR285MC-BH) which is 1393×1040 pixels in full resolution. Its pixel size is 6.4μm. The target images have been captured by the frame rate of 12Hz, the exposure time of 80msec and the camera gain of 20dB.

During the field test in the sunny daytime, an average atmospheric refractive index structure constant (C_n^2) along the slant path was simultaneously measured by a scintillometer (LAS MK II). At that time, the measured Fried

coherence length was 12.7cm at 633nm. The resolutions of USAF bar target are 7.8, 8.8, 9.8, 11.0, 12.4, 13.9 μrad/cycles for each bar elements (E1-E6), respectively. The image of USAF bar target has been resolved in 11.0μrad/cycle on E4. So far, the development of the control algorithm for WFS is still in process. It is shown that resolution enhancement is possible to see more details for the visible image during the sunny daytime.

4. CONCLUSIONS

To obtain the visible image in high resolution, the feedback close-loop AO system has been developed. We have experimentally tested the performances of AO testbed system for the atmospheric seeing conditions such as Fried coherence length and wind speed in the rotating phase plates. Also, in the field tests, we have obtained the high resolution AO images of USAF bar target in visible wavelength ranges after AO compensation in sunny daytime. However, in poor seeing conditions, low image quality has been resulted due to strong turbulence. Mainly, it causes image blurring due to strong scintillations.

REFERENCES

[1] R. K. Tyson, *Principle of adaptive optics*, Academic press, New York, USA, 1991.
[2] J. W. Hardy, *Adaptive Optics for Astronomical Telescopes*, Oxford University, New York, 1998.
[3] L. C. Andrew, *Field Guide to Atmospheric Optics*, SPIE Press, 2004.
[4] F. Roddier, Ed, *Adaptive Optics in Astronomy*, Cambridge University Press, 1999.
[5] K. Stein, S. Gladysz, D. Seiffer and A. Zepp, Atmospheric limitations on the performance of electro-optical system: a brief overview, Proc. of SPIE 9224, 92240U, 2014.
[6] L. C Roberts, et al., IS That Really Your Strehl Ratio?, Proc. of SPIE Vol. 5490, 504 - 515, 2004.
[7] A. Schimpf, M. Mickallef, and J. Charton, 1550Hz Adaptive optics system using commercially available components, Proc. of SPIE Vol. 9148, 914851, 2014.
[8] F. Rooms, S. Camet, and J. Curis, Simultaneous correction of large low order and high order aberrations with a new deformable mirror technology, Proc. of SPIE Vol. 7550, 755027, 2010.
[9] P. Feautrier, and J. L Gach, Visible and Infrared Wavefront Sensing detectors review in Europe-part I, Proceedings of the Third AO4ELT conference, Florence, Italy, 26-31, 2013.
[10] P. Feautrier, *et al.*, Characterization of OCam and CCD220, the fastest and most sensitive camera to date for AO wavefront sensing, Proc. of SPIE Vol. 7736, 77360Z, 2010.
[11] P. Feautrier, *et al.*, The L3Vision CCD220 with its OCam test camera for AO application in Europe, Proc. of SPIE Vol. 7021, 70210C, 2008.